TÜBİTAK

Turkish Journal of Earth Sciences

http://journals.tubitak.gov.tr/earth/

Research Article

Turkish J Earth Sci
(2019) 28: 531-543

doi:10.3906/yer-1903-16

Deep Structure of Central Menderes Massif: data from deep geothermal wells

Fatma GÜLMEZ[1,*], Emre DAMCI[2], Umut Barış ÜLGEN[3], Aral OKAY[4]

[1]Earth Sciences Institute, Johannes Gutenberg University, Mainz, Germany
[2]Sis Enerji Co., İstanbul, Turkey
[3]EG Enerji, İstanbul, Turkey
[4]Department of Geological Engineering, Faculty of Mines, İstanbul Technical University, İstanbul, Turkey

Received: 12.03.2019 • **Accepted/Published Online:** 14.06.2019 • **Final Version:** 22.07.2019

Abstract: The Menderes Massif is a major Alpide metamorphic complex in western Turkey; it is subdivided into southern, central, and northern submassifs by the east-west trending grabens. The basement of the southern Menderes Massif consists of Neoproterozoic micaschists (Selimiye Formation) intruded by Neoproterozoic granites. The basement is overlain by Permo-Carboniferous phyllite, marble, and quartzite (Göktepe Formation), which pass up into a thick sequence of Mesozoic marbles with emery horizons (Milas Marble). The marbles are overlain by latest Cretaceous recrystallized pelagic limestone and Paleocene metaclastics, which are thrusted over by the Lycian nappes. The metamorphism and deformation of the Phanerozoic sequence of the Menderes Massif is Eocene in age. The structure of the central Menderes Massif is controversial with views ranging from an inverted metamorphic sequence to a pile of nappes. Here we report the results from four deep (>3 km) geothermal wells from the central Menderes Massif. Two distinctive lithological units are differentiated in the wells. The top 0.5 to 1 km of the well sections are made up of micaschists, correlated with the Neoproterozoic Selimiye Formation, whereas the lower parts of the wells have cut through graphite-bearing quartzite, phyllite, and marble regarded as being parts of the Göktepe Formation and Milas Marble. The lithological differences are also picked up by a magnetotelluric study, which shows a sharp increase in the conductivity at the contacts of the Selimiye and Göktepe Formations. The question of whether the inversion of the stratigraphic sequence is due to thrusting or recumbent folding is still open.

Key words: Menderes Massif, stratigraphy, geothermal drilling, magnetotellurics

1. Introduction

The Menderes Massif is a large dome-shaped Alpide metamorphic culmination in western Anatolia and constitutes one of the major tectonic units in the Aegean and eastern Mediterranean Regions. Paleogeographically the Menderes Massif is part of the Anatolide-Tauride Block, which was separated from Gondwana during the Triassic through the opening of the southern branch of the Neo-Tethys ocean (Şengör and Yılmaz, 1981). The Anatolide-Tauride Block formed a continental terrane during the Mesozoic between the southern and northern branches of Neo-Tethys. The complete subduction of the northern branch of Neo-Tethys under the Pontides resulted in the Paleocene-early Eocene collision of the Anatolide-Tauride Block with the Pontide Arc. Following this arc-continent collision, the Anatolide-Tauride Block was strongly deformed, and the northern parts were deeply buried and metamorphosed. The Menderes Massif became a distinct tectonic unit as a result of this Eocene regional metamorphism and deformation, and subsequent Miocene domal exhumation (e.g., Şengör et al., 1984). In the south, the Menderes Massif lies tectonically under the Lycian nappes and in the north under the Cycladic Metamorphic Complex and under the uppermost Cretaceous–Paleocene Bornova Flysch Zone (Figure 1). The internal structure of the Menderes Massif is highly debated; the views range from an essentially in situ metamorphic dome to a pile of nappes (e.g., Dürr, 1975; Şengör et al., 1984; Bozkurt and Oberhansli, 2001; Okay, 2001; Ring et al., 1999; Candan et al., 2011a, 2011b). Here we present results from four deep geothermal wells from the Menderes Massif, which shed light on the internal structure of the Menderes Massif.

2. Menderes Massif–stratigraphy and structure

2.1. Southern submassif

The east-west trending Neogene grabens divide the Menderes Massif into three submassifs: the southern, central, and northern submassifs (Figure 1). The geology and stratigraphy of the Menderes Massif is best known from the southern submassif, which forms a southward dipping

* Correspondence: gulmezftma@gmail.com

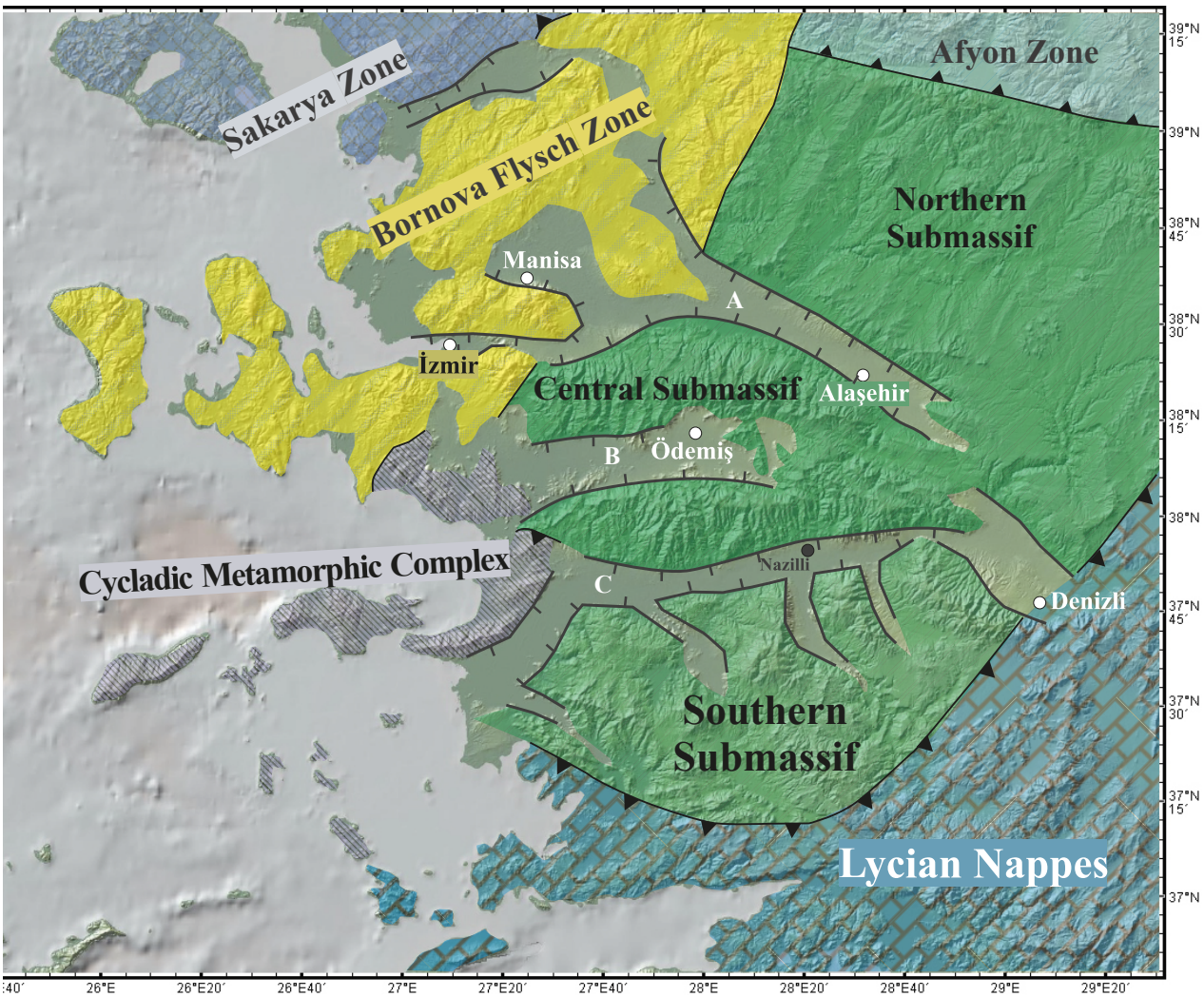

Figure 1. Tectonic map of Western Anatolia (A: Gediz or Alaşehir Graben, B: Küçük Menderes Graben, C: Büyük Menderes Graben).

homocline (Figure 2) with southward decreasing depositional ages and metamorphic grade (Dürr, 1975; Candan et al., 2001, 2011b; Okay, 2001; Whitney and Bozkurt, 2002). The oldest rocks are a thick series of homogenous garnet-micaschists with lenses of garnet-amphibolite. In the Central Submassif, some of the garnet amphibolites contain relicts of granulites and eclogites; the granulite facies metamorphism is dated at ca. 580 Ma and the eclogite facies at 535 Ma (Candan et al., 2001, 2016; Koralay, 2015). In the southern submassif the garnet micaschists, called as the Selimiye Formation, are intruded by voluminous metagranitoids with Late Neoproterozoic–Early Cambrian U-Pb zircon ages of 570 to 520 Ma (Hetzel and Reischmann, 1996; Loos and Reischmann, 1999; Gessner et al., 2004; Koralay et al., 2004; Hasözbek et al., 2010; Koralay et al., 2011, 2012; Koralay, 2015). The Selimiye Formation and the metagranitoids are classically regarded as part of the core of the Menderes Massif, although only the Selimiye Formation has undergone Neoproterozoic deformation and metamorphism; the Ar-Ar mica cooling ages from the metagranitoids are Eocene (Bozkurt and Satır, 2000; Lips et al., 2001; Candan et al., 2011; Koralay et al., 2011), and most of the metagranitoids are posttectonic with respect to the Neoproterozoic orogeny. Next in the stratigraphic sequence are a thick series of intercalated black phyllite, quartzite and dark recrystallized limestone, called the Göktepe Formation. Recrystallized limestones from the Göktepe Formation have yielded Permian and Carboniferous foraminifera from the Göktepe, Karıncalıdağ, Babadağ, and Aydın mountains (Önay,

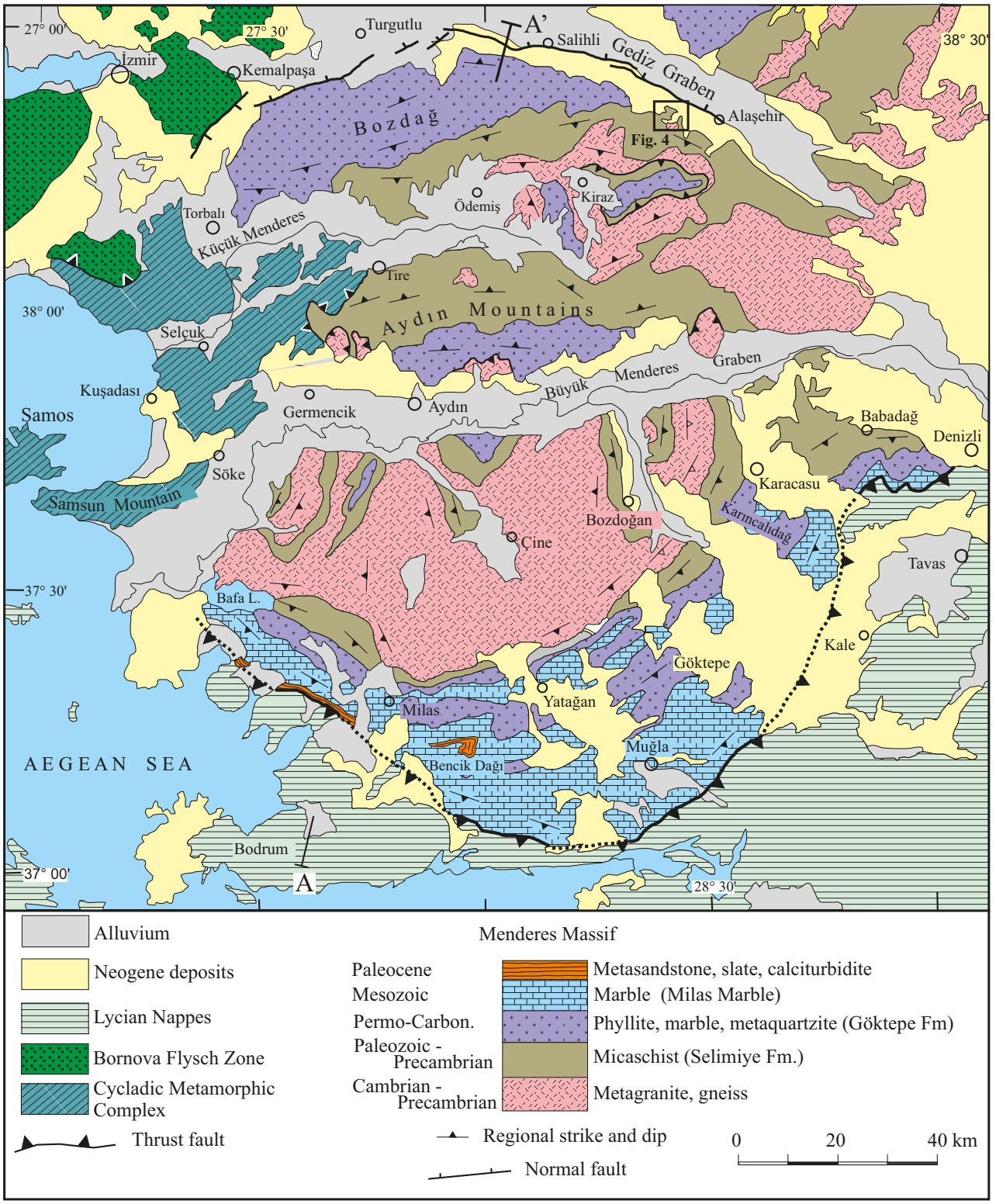

Figure 2. Geological map of the Southern and Central Submassifs of the Menderes Massif based on Konak (2002), Konak and Şenel (2002), and Okay (2001).

1949; Çağlayan et al., 1980; Okay, 2001). The boundary between the Göktepe Formation and the underlying Selimiye Formation or Neoproterozoic metagranitoids is marked by a laterally traceable metaconglomerate and metaquartzite horizon (Candan et al., 2011). The Göktepe Formation is stratigraphically overlain by a thick sequence of carbonates with metabauxite and emery horizons, locally called the Milas Marble. The Milas Marble has yielded Triassic, Jurassic, and Cretaceous algae and foraminifera (Dürr, 1975). The top part of the carbonates contains Upper Cretaceous rudists (Dürr 1975; Özer 1998). The shallow marine, recrystallized carbonates are overlain by recrystallized variegated Upper Cretaceous (Campanian-Maastrichtian) recrystallized pelagic limestone (Kızılağaç Formation) and metaclastics with blocks of serpentinite and Middle Paleocene recrystallized limestone (Kazıklı Formation) marking the end of sedimentation in the Menderes Massif (Figure 3; Dürr, 1975; Çağlayan et al., 1980; Özer et al., 2001). Lycian Nappes, usually with basal Triassic dolomites, lie tectonically over the Kazıklı or Kızılağaç Formations (Figure 2).

The Menderes Massif has undergone two stages of regional metamorphism. The Selimiye Formation contains relics of Neoproterozoic granulite, eclogite to amphibolite facies metamorphism, and the Menderes Massif as a whole, including the Selimiye Formation has undergone an Eocene metamorphism and deformation (e.g., Candan et al., 2001, 2016). The Eocene regional metamorphism in the southern submassif shows a southward decrease in grade ranging from high to low greenschist facies metamorphism (e.g., Whitney and Bozkurt, 2002). The significance of carpholite, discovered at a single locality close to the base of the Göktepe Formation (Whitney et al., 2008) within the framework of the regional metamorphism of the Menderes Massif is controversial.

Despite the well-documented paleontological and biostratigraphic data indicating southward younging of ages, Ring et al. (1999) claimed the existence of several nappes in the southern submassif of the Menderes Massif (Figure 3).

2.2. Central submassif

The formations described from the southern submassif can also be recognized in the central submassif; however, the central submassif has a more complicated structure. It forms a broad synform with the Küçük Menderes Graben at its centre (Figure 2). The core of the synform is constituted by the Neoproterozoic metagranites and the Selimiye Formation, which is underlain by the Göktepe Formation. The Mesozoic carbonates with rudist fossils are present below the Göktepe Formation on the southern part of the central submassif (Özer and Sözbilir, 2003). The interpretation of the contacts between these formations, whether inverted stratigraphic contacts or thrust contacts or both is controversial

3. New data from deep wells

Here we present results from four deep geothermal wells opened in the northern part of the central submassif south of Alaşehir around the village of Soğukyurt. The Soğukyurt area is affected by Eocene deformation and metamorphism and later by extensional faults related to the Miocene exhumation of the Menderes Massif and

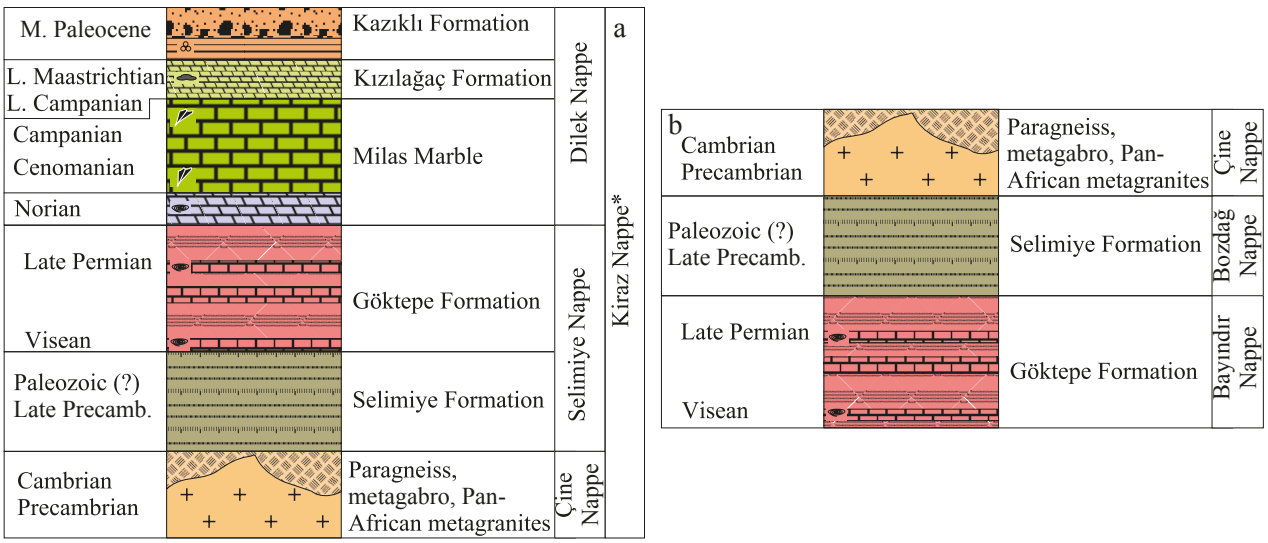

Figure 3. Generalized columnar sections of the a) Southern and b) Central Submassif of the Menderes Massif (Okay, 2001; Dürr, 1975; Hetzel and Reischmann, 1996; Hetzel et al., 1998; Gessner et al., 2001; Gökten et al., 2001). For explanations see the text.

formation of the Gediz Graben. The main rock unit in the Soğukyurt area, below the Miocene sediments, are an alternation of brown to gray, fine-to-medium grained monotonous micaschist and quartzschist with rare marble lenses belonging to the Selimiye Formation (Figure 4). The foliation in the Soğukyurt area dips gently to the south. In the south of Soğukyurt, a small body of metagranite lies tectonically over the micaschists.

Well Sy-23 is one of the deepest geothermal well in Turkey with a bottom hole depth of 4312 m (mMD-meter measured depth) which corresponds to 4070 m true vertical depth (mVTD). The wells were opened by conventional rotary mud drilling and no continuous cores were obtained. Large samples were extracted from the wells by junk basket at irregular intervals, otherwise rock cuttings were studied in every 2 m drilling and described continuously by the well-site geologist. Petrographic thin sections were prepared from the rock cuttings and from large samples at critical intervals.

Simplified logs of the four well are shown in Figure 5. Two main lithological units can be distinguished in the four wells, below the Miocene sedimentary cover. The upper units with a maximum thickness of about 2000 m in the well Sy-24 consists predominantly of light brown

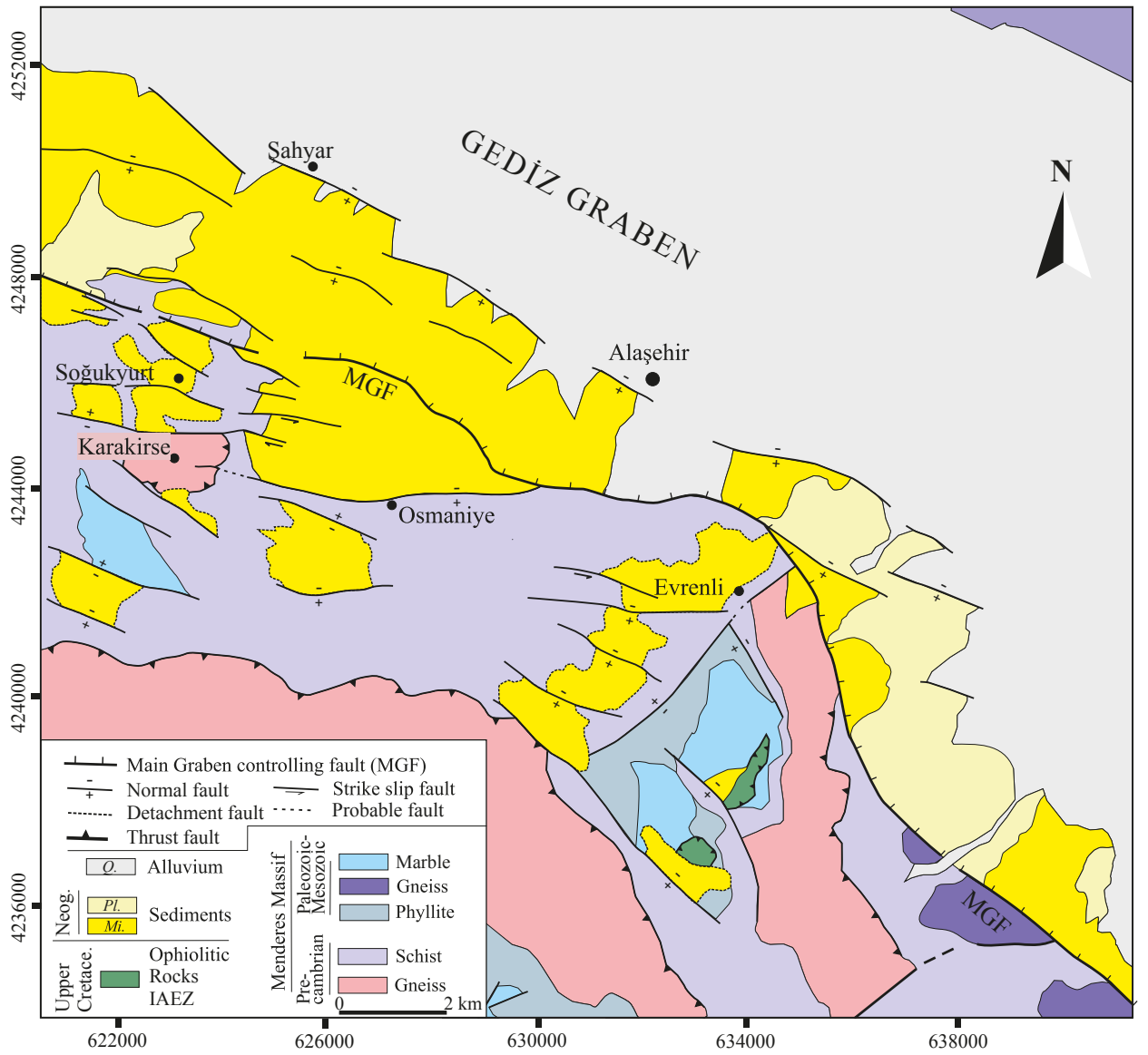

Figure 4. Geological map of the region south of Alaşehir in the Central Submassif of the Menderes Massif compiled from Koralay (2001), Çiftçi and Bozkurt (2009), Candan et al. (2011) and Sunal (2014).

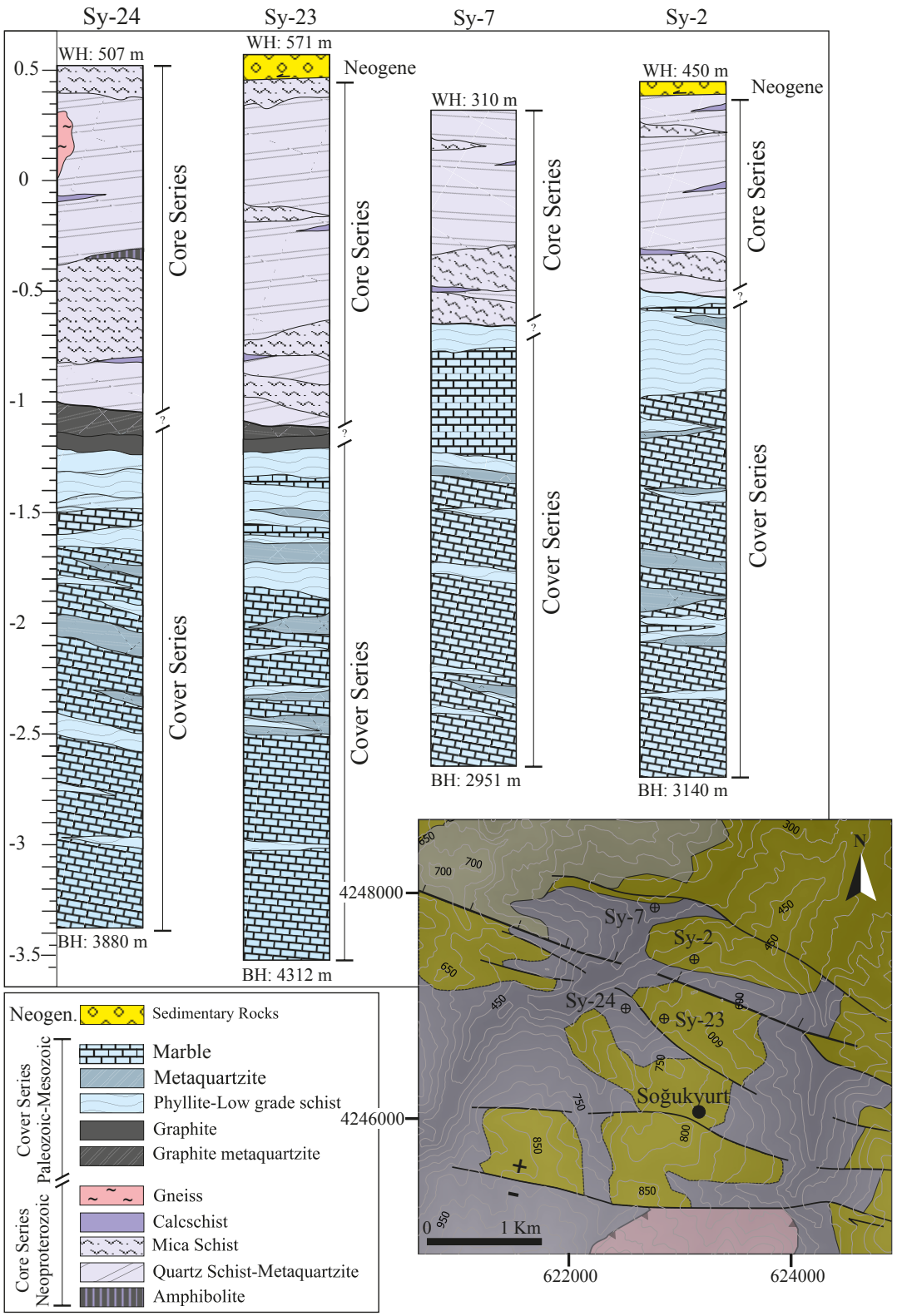

Figure 5. Well logs from Soğukyurt License area. Inset map indicates the well locations (WH: well head elevation from sea level; BH: bottom hole, refers to measured depth of the well).

to light gray mica-schist and quartz-schist with rare local intercalation of calc-schist and graphitic schist. The common mineral assemblage in the mica-schists is quartz + plagioclase + biotite + chlorite + muscovite + opaque minerals ± garnet ± tourmaline ± apatite ± zircon ± calcite (Figures 6a and 6b). Quartz-micaschist is lithologically gradational to the mica-schist and is distinguished by greater amounts of quartz in the rock; calc-schist makes up less than 1% of the upper metamorphic sequence and consists of calcite, quartz, and muscovite. Amphibolite was apparently encountered only at the well Sy-24 well at a depth of 850 m along a zone less than 20-m thick. The hand specimen of amphibolite extracted by junk basket has the mineral assemblage of biotite + hornblende + garnet ± plagioclase + quartz + epidote + sphene ± chlorite ± calcite ± zoisite (Figures 6c and 6d). In the lower levels of the schist series, there is an increase in the amount of metaquartzites. Especially black, graphite-bearing metaquartzites were observed in the wells Sy-24 and Sy-23 (Figure 5). Black metaquartzite samples from the Sy-24 well have the mineral assemblage of quartz + graphite ± sericite ± pyrite (Figures 6e and 6f). Below the black metaquartzites, there is very graphite-rich zone, 10–30 m in thickness.

The schist unit is underlain by a thick sequence of intercalated marble, phyllite, and metaquartzite. This series is significantly softer than metaquartzites evident by the increased rate of penetration (ROP) during the drilling of the wells. The upper part of the marble-phyllite-metaquartzite series is dominated by alternation of dark phyllite, dark marble, and light metaquartzite. In the down section, there is a change to pure white, massif marble with thin intercalation phyllite and metaquartzite. Figure 7 displays down section lithologies. The thickness of the marble-phyllite-metaquartzite series in the well Sy-23 is about 2200 m (Figure 5).

4. Magnetotelluric data

A 5-channel Magnetotelluric (MT) data acquisition system from Phoenix Geophysics Ltd was used to record the MT data at 75 points with approximately 500 m average spacing on an irregular grid due to rough terrain (Figures 8a and 8b). Variations of the Earth's natural electromagnetic field were recorded at each location and analyzed to give estimates of the MT impedance (Egbert, 1997). Full impedance tensor data were inverted within the frequency range from 1000 Hz to 0.003 Hz, and fine cell dimensions were used, having the thinnest cells within the detailed topography. Geoelectric strike directions were computed using both tensor decomposition and induction vectors (McNeice and Jones, 2001). MT Data can exhibit two-dimensional (2D) behavior with the strike direction approximately parallel to the major tectonic boundaries with respect to the Gediz Graben. When the data have a 2D behavior, it is possible to find a 2D solution. However, 3D behavior might usually invalidate the 2D approach and a careful analysis was conducted to ensure that the 2D models were not affected by this. Although there are some static shifts due to local variations indicating that MT data was not spatially aliased, they were removed during 3D MT inversion. 3D MT inversion workflow was designed to provide an estimate of the resistivity distribution up to a depth of by 4 km a.s.l. (Schlumberger, 2014). 3D inversion modelling was carried out using the modified code described priory by Mackie and Madden (1993). The data were edited to mute noisier segments. For the inversion, frequencies greater than 1000 Hz were discarded due to data quality and the depth of the related target. The inversion produced stable structural details at the depths of interest, and a good fit between calculated and observed MT data, with an RMS value of 1.64 for the final inversion.

The upper metamorphic sequence dominated by schist series reveals resistivity values above 100 Ωm, and up to 250 Ωm. There is a sudden decrease of resistivity down to 15 Ωm at the depth of 1000 m below sea-level at Sy-23 and Sy-24 wells, which coincides with the depth to graphite bearing metaquartzites (Figure 8c). The well data show that the lithologies represented by low resistivity values correspond mostly to marbles, phyllite-metaquartzite unit. It is important to note that low resistivity is of a combined outcome of the presence of graphitic zones in metamorphic rocks and geothermal activity in the marble reservoir; hence, it should not be taken as a clear evidence of geothermal activity by itself without a comprehensive evaluation with geologic aspects.

5. Discussion

The deep wells opened on the northern margin of the central submassif indicate the presence of two distinct rock units below the Miocene sediments, in the upper 4 km of the crust. An upper unit dominated by micaschist and quartz-micaschist, and a lower unit consisting mainly of marble, phyllite and quartzite. If we compare these units with the stratigraphy of the Menderes Massif, as known from the Southern submassif, the upper unit can be correlated with the Neoproterozoic Selimiye Formation and the lower unit with Permian-Carboniferous Göktepe Formation and Triassic-Cretaceous Milas Marble. The distinguishing features of the Selimiye Formation are the dominance of thick monotonous micaschists, presence of minor amphibolite and general absence of carbonates, whereas the Göktepe Formation is characterized by an alternation of dark phyllite, marble, and quartzite. Hetzel et al. (1998) previously indicated that Selimiye Formation is distinguished from Göktepe Formation by the occurrence of amphibolites and the absence of marble and quartzite

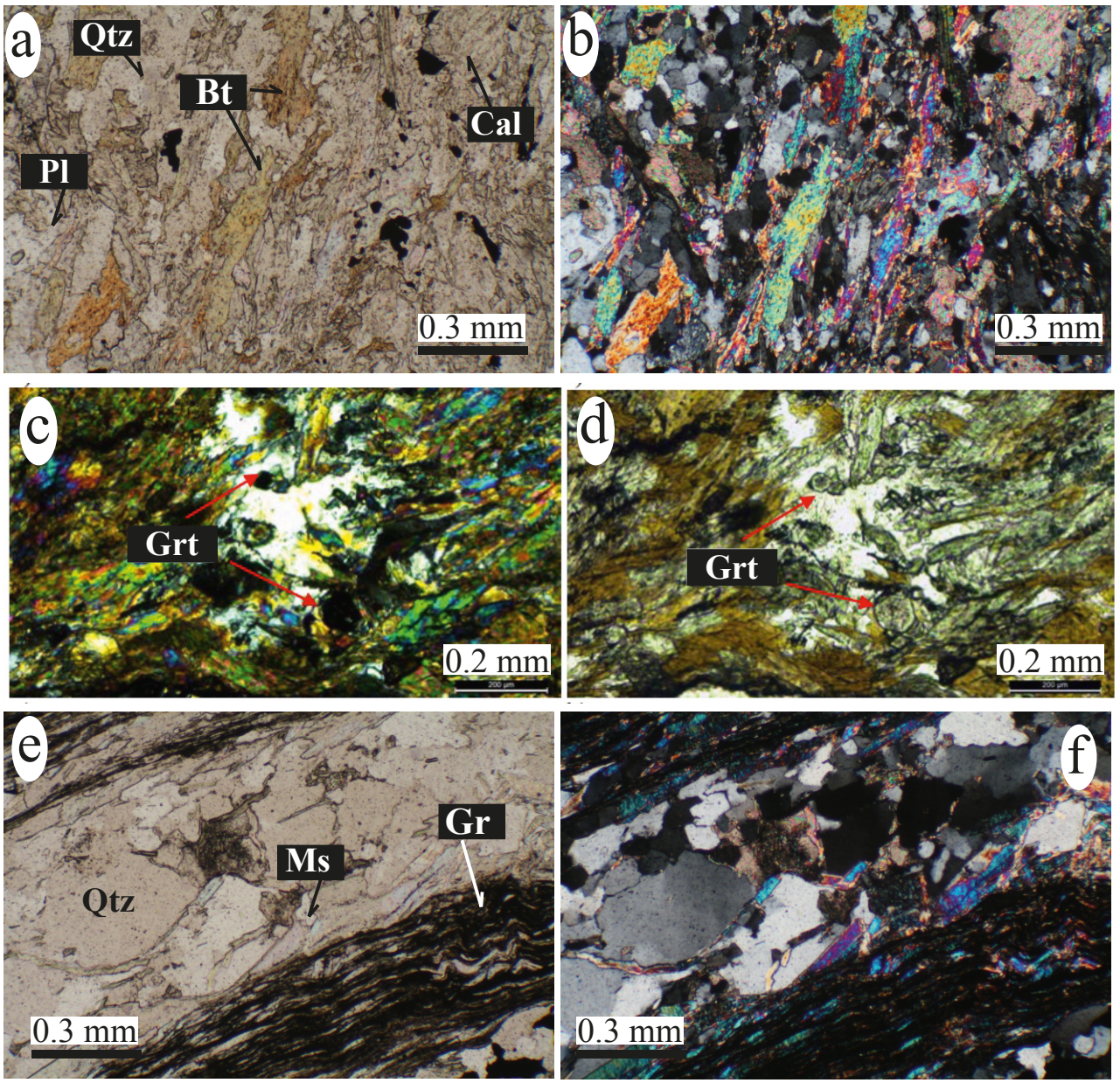

Figure 6. Thin section microphotos of samples from the Soğukyurt wells. Thin section photos of Soğukyurt samples. a-b) lepidoblastic texture by biotite in mica quartz schist under plane and cross polarized light (5× magnification), c-d) garnet bearing amphibolite samples belonging SY-24 well (~1000 m) under cross and plane polarized light (5× magnification), e-f) schistosity in graphite metaquartzites (5× magnification). Qtz: quartz, Pl: plagioclase, Bt: biotite, Cal: calcite, Grt: Granat, Ms: muscovite, Gr: graphite.

intercalations. Especially amphibolites are characteristic for the Neoproterozoic Selimiye Formation (Oberhansli et al., 1997).

The contact between the Selimiye and Göktepe Formations can be taken either at the first appearance of the marble layers in the cores or more likely at the black metaquartzite and graphite-schist layers. The lower parts of the wells Sy-23 and Sy-24 are dominated by massive white marble, which might suggest that this lowermost part belongs to the Mesozoic carbonates of the Menderes Massif.

The MT study shows a sharp change in conductivity corresponding to the boundary of the Selimiye and Göktepe Formations (Figure 8). There are large number of examples where graphite in the rocks causes high conduc-

Figure 7. Various samples from the wellbores a) graphite-bearing marble core from Sy-2 well (~1200 m), b) metaquartzite hand specimen from well Sy-13 (1264 m) with well-developed foliation, c) graphite metaquartzite core from Sy-24 well (1080 m).

tivity (e.g., Santos et al., 2002; Ritter et al., 2005, Kuyumcu et al., 2011; Oohashi et al., 2012), and the presence of graphite is the main reason for the high conductivity in the Göktepe Formation. Graphite in the Permian-Carboniferous Göktepe Formation is most likely of primary origin as shown by the dark color of the rocks of the Göktepe Formation in the field. Carboniferous was a period of carbon accumulation, as witnessed by the coal measures of the Carboniferous throughout the World.

Hydrothermal graphite can be deposited from C-bearing fluids under low pressure and moderate temperature conditions (>350 °C; Ooshashi et al., 2012; Santos et al., 2002). However, in the wells Sy-23 and Sy-24, the static temperature at the graphitic zone is around 135 °C and the maximum calculated reservoir temperature is about 210 °C. The brine samples derived from Soğukyurt wells were all classified as meteoric origin $NaHCO_3$ fluids with relatively high concentrations of noncondensable gas (>1% by weight), which is made up mostly by CO_2 (up to 99%) and minor CH_4 is (max 0.6%). There is no indication of magmatic fluids in the isotopes (Haizlip et al., 2016). Therefore, a hydrothermal origin of graphite can be ruled out for the Soğukyurt area.

It is difficult to characterize the nature of the contact between the Selimiye and Göktepe Formations based on the well cuttings. The sharp change in the electrical conductivity and the presence of graphite-rich zone at about one kilometer depths in the wells Sy-23 and Sy-24 might suggest a shear zone, since graphite is a common fault gouge component due to its ability to lower the friction as a dry lubricant in the brittle upper crust (Summers and Byerlee, 1977; Manatschal, 1999; Craw and Upton, 2014). However, the permeability along this graphite-rich zone is extremely low, as shown by the well tests with no recorded mud loss or fluid entry during flow tests; in the Sy-24 well the highly fractured permeable zone lies at depth of 3000 m, approximately 1400 m deeper than the graphitic zone. There are two possibilities regarding the nature of the

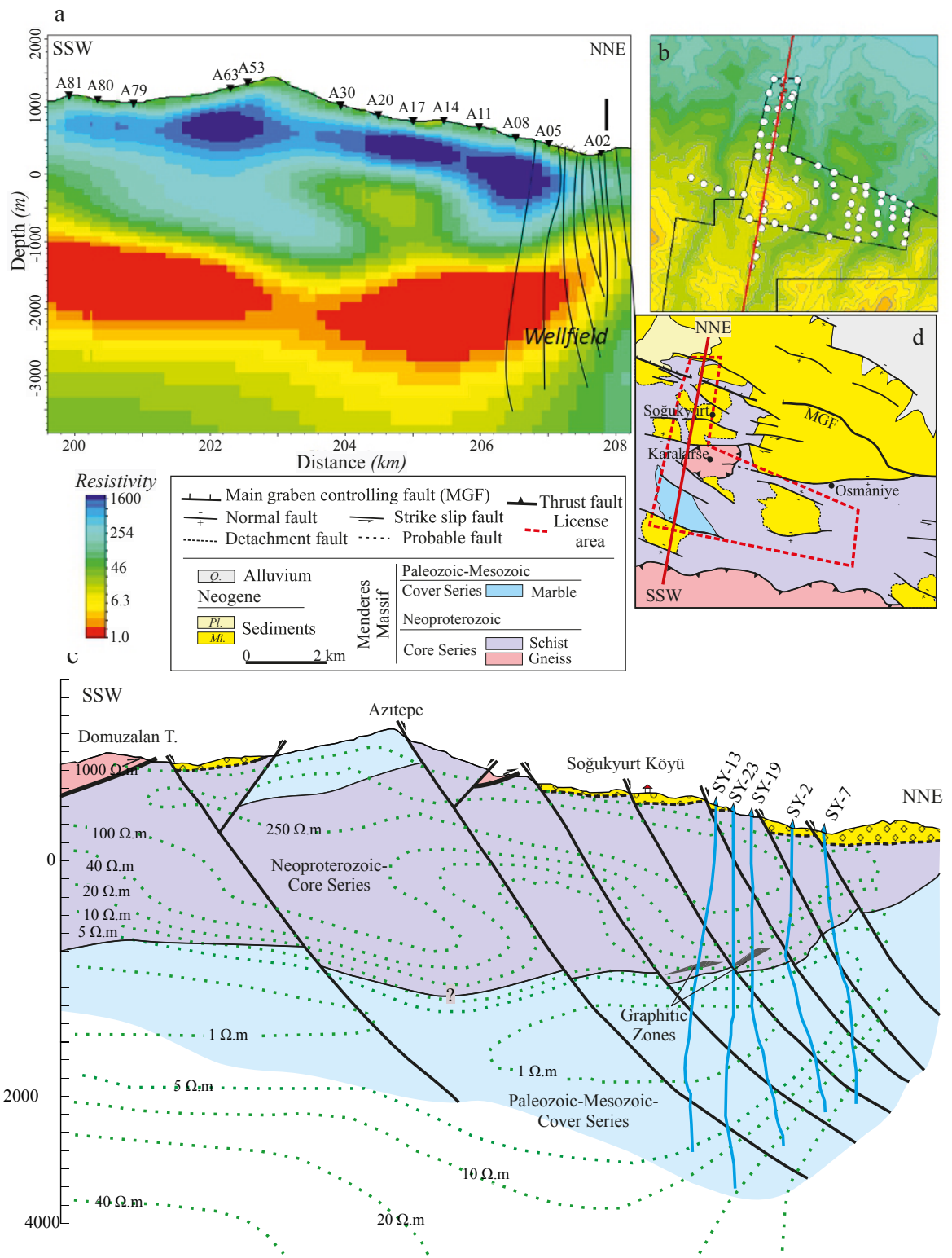

Figure 8. a) South-southwest to north-northeast cross section of 3-D inversion MT resistivity model with well tracks (for explanations please see text), b) Magnetotelluric station locations superimposed on a topographic cross-section of the Soğukyurt License area, c) Interpreted vertical cross-section of Soğukyurt license area after combining magnetotelluric data with lithologic findings, d) geological map implying direction of cross section.

contact between the Selimiye and Göktepe Formations as observed in the wells. The contact can be an inverted stratigraphic contact, as described in the Aydın mountains (Okay, 2001) or a deep-seated shear zone. With the available data, it is not possible to reach a firm conclusion about the nature of the contact.

5.Conclusions

Results from four deep wells opened on the northern margin of the central submassif south of Alaşehir indicate the presence 2-km thick phyllite-marble-metaquartzite series overlain by 1.5- to 2-km-thick sequence of micaschists. The phyllite-marble-metaquartzite series is correlated with the Permian-Carboniferous Göktepe Formation and Triassic-Cretaceous Milas Marble and the overlying micaschists with the Neoproterozoic Selimiye Formation. These two formations are also clearly imaged in the MT profiles, where the graphite-rich Göktepe Formation exhibits a high electrical conductivity compared to the Selimiye Formation. There is no evidence for a brittle thrust fault between the Selimiye and Göktepe formations in the wells. The nature of the contact, whether an inverted stratigraphic contact or a deep-seated ductile shear zone, remains to be studied.

Acknowledgments

We greatly appreciate the Özmen Holding for their contributions to Turkey's geology by providing well log data. Special thanks to well-site geologists Gökhan Toru, Ertan Göllü, Mustafa Uysal for their skilled assistance during drilling operations and geophysicist Tuba Kara. We greatly appreciate the discussions with Osman Candan and Ersin Koralay on an early version of the manuscript. We would like to thank the editor Orhan Tatar and three anonymous reviewers for their valuable comments which clearly improved the paper.

References

Bozkurt E, Satir M. (2000). The southern Menderes Massif (western Turkey): geochronology and exhumation history. Geological Journal 35 (3-4): 285-296.

Bozkurt E, Oberhänsli R. (2001). Menderes Massif (Western Turkey): structural, metamorphic and magmatic evolution–a synthesis. International Journal of Earth Sciences, 89 (4): 679-708.

Candan O, Dora O, Oberhänsli R, Çetinkaplan M, Partzsch J et al. (2001). Pan-African high-pressure metamorphism in the Precambrian basement of the Menderes Massif, western Anatolia, Turkey. International Journal of Earth Sciences 89 (4): 793-811.

Candan O, Dora ÖO, Oberhanslı R, Koralay E, Çetinkaplan M et al. (2011a). Stratigraphy of the pan - african basement of the menderes massif and the relationship with late neoproterozoic/cambrian evolution of the gondwana. Bulletin of the Mineral Research and Exploration 142: 25-68.

Candan O, Oberhanslı R, Akal OÖ (2011b). Polymetamorphic evolution of the Pan-African Basement and Palaeozoic–Early tertiary cover series of the Menderes Massif. Bulletin of the Mineral Research and Exploration 142: 121-165.

Candan O, Koralay OE, Topuz G, Oberhänsli R, Fritz H, et al. (2016). Late Neoproterozoic gabbro emplacement followed by early Cambrian eclogite-facies metamorphism in the Menderes Massif (W. Turkey): implications on the final assembly of Gondwana. Gondwana Research 34: 158-173.

Craw D, Upton P (2014). Graphite reaction weakening of fault rocks, and uplift of the Annapurna Himal, central Nepal. Geosphere 10 (4): 720-731.

Çağlayan A, Öztürk EM, Öztürk S, Sav H, Akat U. (1980). Some new data on the southern part of the Menderes massif and a structural interpretation. Jeoloji Mühendisliği 10: 9-17 (article in Turkish with an English abstract).

Çiftçi NB, Bozkurt E (2009). Evolution of the Miocene sedimentary fill of the Gediz Graben, SW Turkey. Sedimentary Geology 216 (3-4): 49-79.

Dürr SH (1975). Über alter und geotektonische Stellung des Menderes-Kristallins, SW-Anatolien und seine Aequivalente in der mittleren Aegaeis. Habil.-Schr. Philipps-Univ. Marburg/Lahn (article in German).

Egbert GD (1997). Robust multiple-station magnetotelluric data rocessing. Geophysical Journal International 130 (2): 475-496.

Gessner K, Collins AS, Ring U, Güngör T (2004). Structural and thermal history of poly-orogenic basement: U–Pb geochronology of granitoid rocks in the southern Menderes Massif, Western Turkey. Journal of the Geological Society 161 (1): 93-101.

Gokten E, Havzoğlu T, Şan Ö (2001). Tertiary evolution of the central Menderes Massif based on structural investigations of metamorphics and sedimentary cover rocks between Salihli and Kiraz (western Turkey). International Journal of Earth Sciences 89 (4): 745-756.

Hasözbek A, Akay E, Erdoğan B, Satır M, Siebel W (2010). Early Miocene granite formation by detachment tectonics or not? A case study from the northern Menderes Massif (Western Turkey). Journal of Geodynamics 50 (2): 67-80.

Haizlip JR, Stover MM, Garg SK, Haklidir FT, Prina N (2016). Origin and impacts of high concentrations of carbon dioxide in geothermal fluids of western Turkey. In: Proceedings, 41st Workshop on Geothermal Reservoir Engineering Stanford University. Stanford, CA, USA. pp. 1302-1313.

Hetzel R, Reischmann T (1996). Intrusion age of Pan-African augen gneisses in the southern Menderes Massif and the age of cooling after Alpine ductile extensional deformation. Geological Magazine 133 (5), 565-572.

Hetzel R, Romer RL, Candan O, Passchier CW (1998). Geology of the Bozdag area, central Menderes massif, SW Turkey: Pan-African basement and Alpine deformation. Geologische Rundschau 87 (3): 394-406.

Konak N (2002). Türkiye jeoloji haritası, İzmir paftası 1: 500 000. Maden Tetkik ve Arama Genel Müdürlüğü, Ankara (in Turkish).

Konak N. Şenel M (2002). Türkiye jeoloji haritası, Denizli paftası 1: 500 000. Maden Tetkik ve Arama Genel Müdürlüğü, Ankara (in Turkish).

Koralay OE (2001). Geology, geochemistry and geochrology of granitic and leucocratic ortogneisses at the eastern part of Ödemiş-Kiraz Submassif: Pan-African and Triassic magmatic activities. PhD, Dokuz Eylül University, İzmir, Turkey.

Koralay OE, Dora OÖ, Chen F, Satir M, Candan O (2004). Geochemistry and geochronology of orthogneisses in the Derbent (Alaşehir) area, eastern part of the Ödemiş-Kiraz submassif, Menderes Massif: Pan-African magmatic activity. Turkish Journal of Earth Sciences 13(1): 37-61.

Koralay OE, Candan O, Akal C, Dora OÖ, Chen F et al. (2011). The geology and geochronology of the pan-african and triassic metagranitoids in the menderes massif, western anatolia, turkey. Bulletin of the Mineral Research and Exploration 142: 69-121.

Koralay OE, Candan O, Chen F, Akal C, Oberhänsli R et al. (2012). Pan-African magmatism in the Menderes Massif: geochronological data from leucocratic tourmaline orthogneisses in western Turkey. International Journal of Earth Sciences 101 (8): 2055-2081.

Koralay OE (2015). Late Neoproterozoic granulite facies metamorphism in the Menderes Massif, Western Anatolia/Turkey: implication for the assembly of Gondwana. Geodinamica Acta 27 (4): 244-266.

Kuyumcu ÖC, Destegül Solaroğlu UZ, Hallinan S, Turkoglu E, Soyer W (2012). Interpretation of 3D Magnetotelluric (MT) surveys; basement conductors of the Menderes Massif, Western Turkey. In: International Geophysical Conference and Oil & Gas Exhibition; İstanbul, Turkey. pp. 1-4.

Lips AL, Cassard D, Sözbilir H, Yilmaz H, Wijbrans JR (2001). Multistage exhumation of the Menderes massif, western Anatolia (Turkey). International Journal of Earth Sciences 89 (4): 781-792.

Loos S, Reischmann T (1999). The evolution of the southern Menderes Massif in SW Turkey as revealed by zircon dating. Journal of the Geological Society 156 (5): 1021-1030.

Manatschal G (1999). Fluid-and reaction-assisted low-angle normal faulting: evidence from rift-related brittle fault rocks in the Alps (Err Nappe, eastern Switzerland). Journal of Structural Geology 21 (7): 777-793.

Mackie RL, Madden TR, Wannamaker P (1993). '3-D Magnetotelluric Modeling Using Difference Equations – Theory and Comparisons to Integral Equation Solutions. Geophysics 58: 215-226.

McNeice GW, Jones AG (2001). Multisite, multifrequency tensor decomposition of magnetotelluric data. Geophysics 66 (1): 158-173.

Oberhänsli R, Candan O, Dora OÖ, Dürr StH (1997). Eclogites within the Menderes massif/western Turkey. Lithos 41 (1-3): 135-150.

Okay AI (2001). Stratigraphic and metamorphic inversions in the central Menderes Massif: a new structural model. International Journal of Earth Sciences 89 (4): 709-727.

Oohashi K, Hirose T, Kobayashi K, Shimamoto T (2012). The occurrence of graphite-bearing fault rocks in the Atotsugawa fault system, Japan: Origins and implications for fault creep. Journal of Structural Geology 38: 39-50.

Önay TŞ (1949). Über die Smirgelgesteine Südwest-Anatoliens. Schweizerische Mineralogische und Petrographische Mitteilungen, 29: 357-492 (article in German).

Özer S (1998). Rudist bearing Upper Cretaceous metamorphic sequences of the Menderes Massif (Western Turkey). Geobios 31: 235-249.

Özer S, Sözbilir H, Özkar İ, Toker V, Sari, B (2001). Stratigraphy of Upper Cretaceous–Palaeogene sequences in the southern and eastern Menderes Massif (western Turkey). International Journal of Earth Sciences 89 (4): 852-866.

Özer S, Sözbilir H (2003). Presence and tectonic significance of Cretaceous rudist species in the so-called Permo-Carboniferous Göktepe Formation, central Menderes metamorphic massif, western Turkey. International Journal of Earth Sciences 92 (3): 397-404.

Ring U, Laws S, Bernet M (1999). Structural analysis of a complex nappe sequence and late-orogenic basins from the Aegean Island of Samos, Greece. Journal of Structural Geology 21 (11): 1575-1601.

Ritter O, Hoffmann-Rothe A, Bedrosian PA, Weckmann U, Haak V (2005). Electrical conductivity images of active and fossil fault zones. Geological Society, London, UK: Special Publications 245 (1): 165-186.

Santos FAM, Mateus A, Almeida EP, Pous J, Mendes Victor LA (2002). Are some of the deep crustal conductive features found in SW Iberia caused by graphite? Earth and Planetary Science Letters 201 (2): 353-367.

Schlumberger (2014). 3D Modelling of Magnetotelluric Data, Area 74 Alaşehir. Milan, Italy: Schlumberger, Integrated EM Center of Excellence.

Summers R, Byerlee J (1977). A note on the effect of fault gouge composition on the stability of frictional sliding. In: International Journal of Rock Mechanics and Mining Sciences and Geomechanics Abstracts 14 (3): 155-160.

Sunal G (2014). Alaşehir Güneyine (İzmir L20-B3 Paftasına) Dair Jeolojik Rapor. Özmen Holding, İstanbul (in Turkish).

Şengör AMC, Yilmaz Y (1981). Tethyan evolution of Turkey: a plate tectonic approach. Tectonophysics 75 (3-4): 181-241.

Şengör AMC, Satir M, Akkök R (1984). Timing of tectonic events in the Menderes Massif, western Turkey: Implications for tectonic evolution and evidence for Pan-African basement in Turkey. Tectonics 3 (7): 693-707.

Whitney DL, Bozkurt, E (2002). Metamorphic history of the southern Menderes massif, western Turkey. Geological Society of America Bulletin 114 (7): 829-838.

Whitney DL, Teyssier C, Kruckenberg SC, Morgan VL, Iredale LJ (2008). High-pressure–low-temperature metamorphism of metasedimentary rocks, southern Menderes Massif, western Turkey. Lithos 101 (3-4): 218-232.